electronics

Article

A Gysel Power Divider/Combiner with Enhanced Power-Handling Capability

Chao Fu [1,2], Tianwei He [1], Wenrao Fang [2,*], Wenhua Huang [2], Ruyu Fan [1], Lulu Wang [2], Yuchuan Zhang [2] and Yu Cao [2]

[1] Department of Engineering Physics, Tsinghua University, Beijing 100084, China
[2] Science and Technology on High Power Microwave Laboratory, Northwest Institute of Nuclear Technology, Xi'an 710024, China
* Correspondence: fangwenrao@nint.ac.cn; Tel.: +86-029-84767843

Abstract: By increasing the impedance of the microstrip of the combine port, a new Gysel power combiner/divider (PCD) with enhanced average power-handling capability (APHC) was proposed. This article shows the simulated results of the traditional Gysel PCD and the proposed Gysel PCD at the center frequency of 2.4 GHz and 10 GHz. For verification, one example of the proposed Gysel PCD operating at 2.4 GHz was designed, fabricated, and measured. One traditional Gysel PCD operating at 2.4 GHz was also fabricated to compare the APHC of the proposed Gysel PCD and the traditional Gysel PCD, by means of measuring the temperature variation of the microstrip line at the same power. The measurement result suggests the APHC of the proposed Gysel PCD is nearly twice that of the traditional Gysel PCD.

Keywords: Gysel; power combiner/divider; impedance; combine port; average power-handling capability

check for updates

Citation: Fu, C.; He, T.; Fang, W.; Huang, W.; Fan, R.; Wang, L.; Zhang, Y.; Cao, Y. A Gysel Power Divider/Combiner with Enhanced Power-Handling Capability. *Electronics* **2022**, *11*, 2660. https://doi.org/10.3390/electronics11172660

Academic Editor: Ahmed Abu-Siada

Received: 31 July 2022
Accepted: 24 August 2022
Published: 25 August 2022

1. Introduction

The power combiner/divider is an essential passive component in modern radar and microwave communication systems. The Gysel PCD is a popular structure for its simplicity in structure, low insertion loss, and good isolation [1,2]. The current research mainly focuses on improving the isolation or bandwidth of the Gysel PCD [3–5], and there is less research on the improvement of the power-handling capability of the Gysel PCD. The maximum average power-handling capability of the microstrip Gysel PCD can be determined by the heating in the materials of microstrip lines (related to the ohmic and dielectric losses). The APHC of microstrip lines was first studied by Gupta, K.C. [6,7]. Later on, different works dealt with APHC for microstrip coupled lines [8,9], coupled-line filters [10,11], filters [12,13], multilayer microstrip lines [14], and thin-film microstrip lines [15–17], and there is no research on the APHC of the Gysel PCD from the point of view of the power-handling capacity of the microstrip line. As far as the authors know, the current research on improving the APHC of the Gysel PCD is mainly by increasing the power capacity of the isolation resistors or the number of the isolation resistors [18–20], and no research that dealt with the power-handling capacity of the microstrip has been reported.

This article reports a microstrip Gysel PCD with a high impedance of the combine port and high APHC. The simulated results prove that the proposed Gysel PCD has good power distribution and isolation functions for 2.4 GHz and 10 GHz. Thermal characterization measurement results of the traditional and the proposed Gysel PCD at 2.4 GHz implemented on the microstrip are provided validating the proposed method.

2. Design Theory and Circuit Structure

The generated heat in the microstrip produces a gradient of temperature per unit of power ΔT_0 (°C/W) between the strip and the ground plane limiting the maximum APHC. The ΔT_0 can be calculated as [5]

$$\Delta T_0 = \Delta T_c + \Delta T_d = \frac{2h(\alpha_c + \alpha_d)}{K \times W_e} \tag{1}$$

where ΔT_c and ΔT_d are the temperature gradients generated in the microstrip due to conductor and dielectric losses, K is the thermal conductivity of the substrate, α_c and α_d are the conductor and dielectric attenuation constants (in Np/m), and α_c and α_d are relevant to the thickness t of the strip and the thickness h of the substrate. W_e is the thermal effective microstrip width based on a parallel plate waveguide model and can be calculated as [7]

$$\Delta W_e = \frac{120\pi h}{Z \times \sqrt{\varepsilon_r}} \tag{2}$$

Z and ε_r are the impedance and effective dielectric constant of the microstrip. Combing (1) and (2), (3) can be derived as

$$\Delta T_0 = \Delta T_c + \Delta T_d = \frac{(\alpha_c + \alpha_d) \times \sqrt{\varepsilon_r} \times Z}{60\pi K} \tag{3}$$

Once ΔT_0 is known, the APHC is obtained as

$$P_{\max} = \frac{T_{\max} - T_{amb}}{\Delta T_0} = \frac{60\pi(T_{\max} - T_{amb})K}{Z \times (\alpha_c + \alpha_d) \times \sqrt{\varepsilon_r}} \tag{4}$$

T_{max} is the maximum temperature which can be defined as the temperature at which the circuit changes its electrical or mechanical performance. T_{amb} is set as a given constant temperature which is generally the ambient temperature. K, α_c, α_d, and ε_r are constants when the conductor and dielectric are the same, while h and t are fixed. Therefore, the ΔT_0 is proportional to Z, and P_{max} is inversely proportional to Z.

Figure 1 shows the traditional microstrip Gysel PCD connected with Z_0 = 50 Ω character impedance and two load resistors R_L = 50 Ω connecting to the ground plane. The traditional microstrip Gysel PCD is made up of seven lines, and the electrical length θ_0 of these lines is 90° at the center frequency.

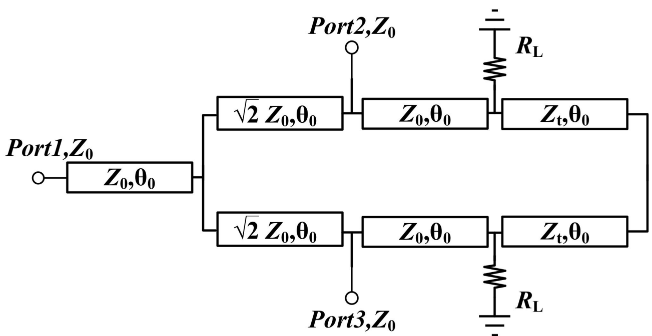

Figure 1. Traditional microstrip Gysel PCD.

For the traditional microstrip Gysel PCD, the impedance of the microstrip of divide ports and the combine port is equal, and therefore, the power of the combine port will reach its APHC while the power of divide ports will only reach half of the APHC. The APHC of the combine port will limit the APHC of the traditional microstrip Gysel PCD, and therefore, the APHC of the microstrip Gysel PCD can be improved by increasing the impedance of the microstrip of the combine port.

Figure 2a shows the proposed microstrip Gysel PCD connected with two load resistors R_L. As previously analyzed, the APHC of the microstrip is inversely proportional to Z, and the power passing through the combine port is always twice that of divide ports; therefore, it would be reasonable to set Z_1 to $Z_0/2$. If Z_1 is greater than $Z_0/2$, the APHC of the combine port will limit the APHC of the proposed Gysel PCD; if Z_1 is lower than $Z_0/2$, the APHC of divide ports will limit the APHC of the proposed Gysel PCD. The typical even–odd mode method was used to obtain the explicit closed-form equations, which determine the parameters (Z_2, Z_3, Z_4, and R_L, and the symbol of admittance is $Y = 1/Z$, $G = 1/R$).

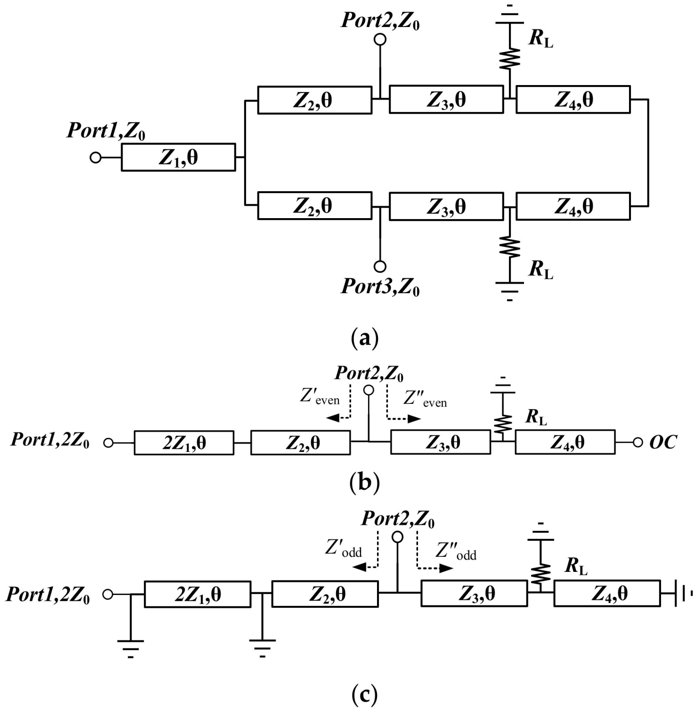

Figure 2. The proposed microstrip Gysel PCD and the even/odd mode circuit of the proposed microstrip Gysel PCD. (**a**) The proposed microstrip Gysel PCD. (**b**) The even-mode circuit. (**c**) The odd-mode circuit.

Figure 2b shows the equivalent circuit of the proposed Gysel PCD under the even-mode excitation. The center vertical plane is equivalent to a virtual magnetic wall. The impedance of port 1 is doubled. The admittances relation can be formulated and expressed by (5)–(7):

$$Y_{even} = Y'_{even} + Y''_{even} \tag{5}$$

$$Y'_{even} = Y_2 \frac{\frac{Y_1}{2}\frac{Y_0 + jY_1\tan\theta}{Y_1 + jY_0\tan\theta} + jY_2\tan\theta}{Y_2 + j\frac{Y_1}{2}\frac{Y_0 + jY_1\tan\theta}{Y_1 + jY_0\tan\theta}\tan\theta} \tag{6}$$

$$Y''_{even} = Y_3 \frac{G_L + jY_4\tan\theta + jY_3\tan\theta}{Y_3 + j(G_L + jY_4\tan\theta)\tan\theta} \tag{7}$$

At the center frequency (θ = 90°), to achieve good impedance matching, Y_{even} is equal to Y_0. According to (5)–(7), we can obtain

$$Y_{even} = \frac{2Y_2^2 Y_0}{Y_1^2} = Y_0 \tag{8}$$

$$Z_2 = \sqrt{2} \times Z_1 = 25\sqrt{2}\Omega \tag{9}$$

Figure 2c shows the equivalent circuit of the proposed Gysel PCD under the odd-mode excitation. In this case, port 1 can simply form a short circuit since the center vertical plane is equivalent to a virtual electric wall. The odd-mode admittance at port 2 can be expressed by (10)–(12):

$$Y_{odd} = Y'_{odd} + Y''_{odd} \tag{10}$$

$$Y'_{odd} = -jY_2 \cot\theta \tag{11}$$

$$Y''_{odd} = Y_3 \frac{G_L - jY_4 \tan\theta + jY_3 \tan\theta}{Y_3 + j(G_L - jY_4 \tan\theta)\tan\theta} \tag{12}$$

To achieve a perfect match and isolation between port 1 and port 2 at the center frequency, Y_{odd} is equal to Y_0. Then, we obtain the results as

$$Y_{odd} = \frac{Y_3^2}{2G_L} = Y_0 \tag{13}$$

$$Z_3 = 50\Omega \tag{14}$$

Note that Z_3 does not influence the impedance matching at the center frequency. For a wider frequency band, we choose a lower value of Z_3 = 35 Ω.

As discussed above, divide ports and the combine port of the proposed Gysel PCD will be matched at the center frequency.

3. Implementation and Measurement

3.1. Prototypes for Traditional Gysel PCD and Proposed Gysel PCD

To verify the proposed design theory, this study used the Advanced Design System to simulate the performance of the traditional Gysel PCD and the proposed Gysel PCD at the center frequency of 2.4 GHz and 10 GHz. To validate the proposed method, a traditional Gysel PCD and a proposed Gysel PCD at 2.4 GHz were fabricated. The circuits were designed and implemented on a Rogers5880 substrate with a relative dielectric constant of 2.2 and a thickness of 0.508 mm, and the thickness of the metal layer was 17.5 µm. The manufacturer of the substrate is Rogers Corporation from Chandler, Arizona, USA. Chip resistors and bent microstrip lines were used to decrease the size of the fabricated circuits. The parameter values of the proposed PCD were Z_1 = 25 Ω, Z_2 = 35.35 Ω, Z_3 = 50 Ω, Z_4 = 35 Ω, and R_L = 50 Ω. Figure 3a,b shows the layouts of the fabricated traditional Gysel PCD and fabricated proposed Gysel PCD, respectively. The fabricated traditional Gysel PCD had a length of 64 mm and a width of 34 mm, and the fabricated proposed Gysel PCD had a length of 64 mm and a width of 41 mm. The measurement was carried out on a network analyzer.

Figure 4a,b show the simulated S-parameters of the proposed Gysel PCD at the center frequency of 2.4 GHz and 10 GHz, respectively. S21 represents the isolation between divide ports, S31 represents the insertion loss between one divide port and the combine port, S33 represents the return loss of the combine port, and S11 represents the return loss of one divide port. The measured isolation is better than 15 dB from 2.31 to 2.65 GHz, and the measured return loss is better than 20 dB from 2.31 GHz to 2.47 GHz. The measured insertion loss S31 is 3.21 dB. The simulation results show that the proposed Gysel PCD has good isolation and insertion loss at the center frequency of both 2.4 GHz and 10 GHz. Figure 4c shows the measured S-parameters of the fabricated proposed Gysel PCD. The measured isolation S21 is better than 15 dB from 2.11 to 2.67 GHz, and the measured return loss S33 is better than 20 dB from 2.31 GHz to 2.47 GHz. The measured insertion loss S21 at the center frequency is less than 3.21 dB.

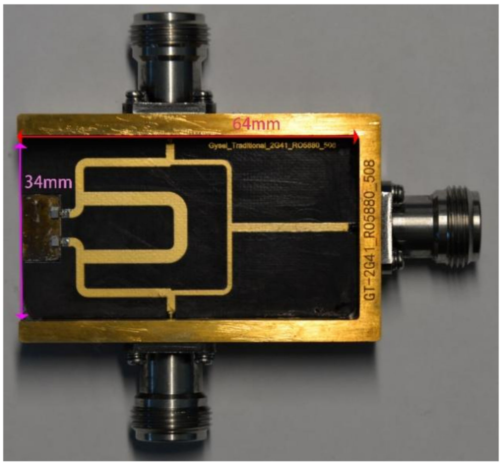

(**a**)

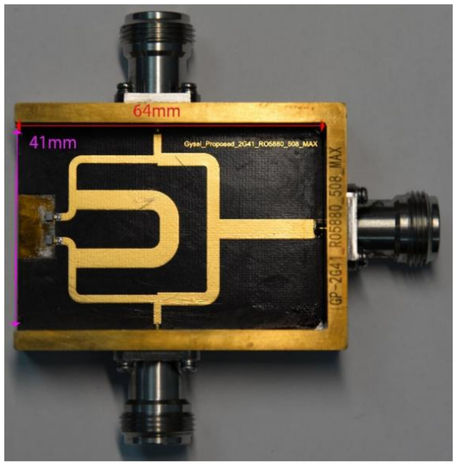

(**b**)

Figure 3. The fabricated traditional Gysel PCD and the fabricated proposed Gysel PCD. (**a**) The fabricated traditional Gysel PCD. (**b**) The fabricated proposed Gysel PCD.

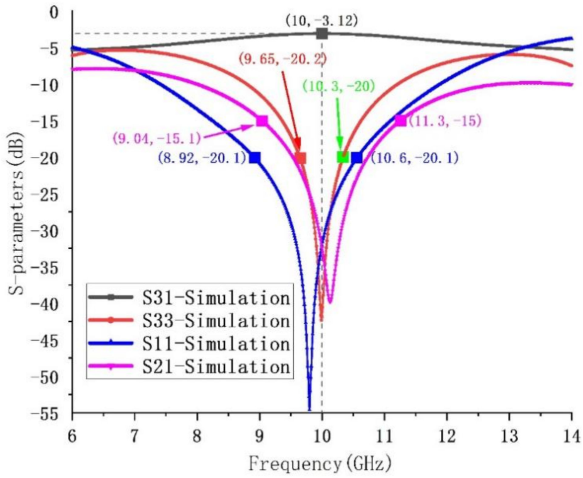

(**b**)

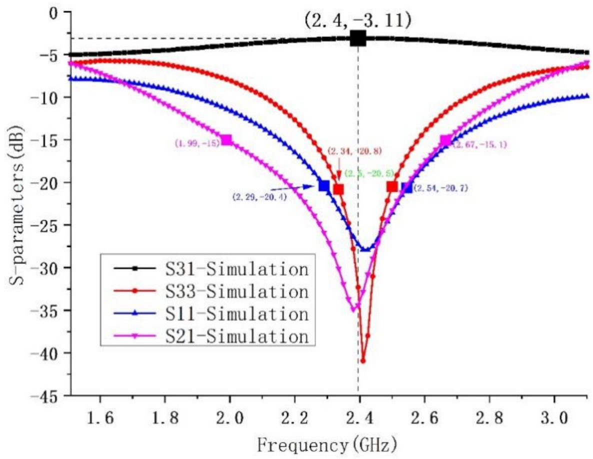

(**a**)

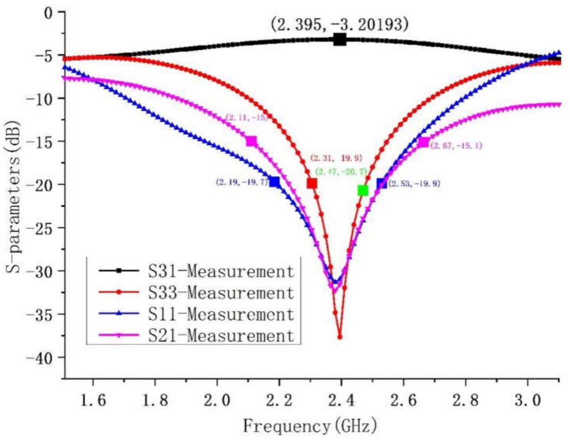

(**c**)

Figure 4. (**a**) The simulated S-parameters of the fabricated proposed Gysel PCD at the center frequency of 2.4 GHz. (**b**) The simulated S-parameters of the fabricated proposed Gysel PCD at the center frequency of 10 GHz. (**c**) The measured S-parameters of the fabricated proposed Gysel PCD at the center frequency of 2.4 GHz.

Figure 5 shows the measured S-parameters of the traditional Gysel PCD and the proposed Gysel PCD. S31 represents the insertion loss between one divide port and the combine port, and S33 represents the return loss of the combine port. The insertion loss S31 of the traditional Gysel PCD and the proposed Gysel PCD is nearly the same at the center frequency.

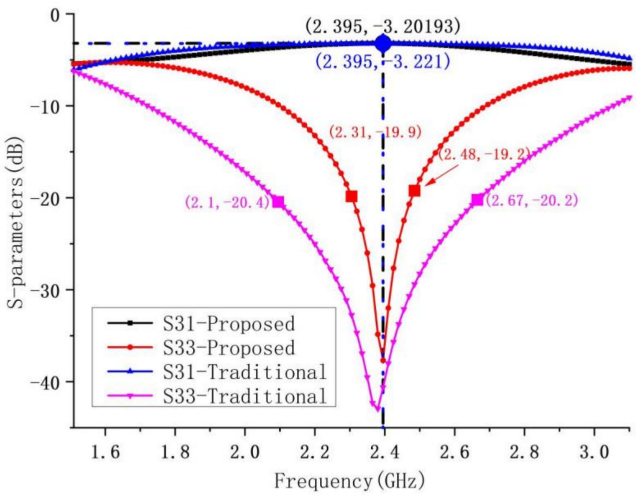

Figure 5. Measured S-parameters of the traditional Gysel PCD and the proposed Gysel PCD.

3.2. Thermal Characterization Measurement Experimental Results and Analysis

To verify the proposed design, a thermal characterization measurement setup was arranged to measure the thermal profile of the device with an infrared camera for the traditional Gysel PCD and the proposed Gysel PCD. Figure 6a shows the measurement setup for thermal characterization of the device under test (DUT). Figure 6b shows the photograph of one of the DUTs. The DUT is suspended above the table so that all its layers are subject to natural convection. Since the infrared camera measures thermal radiation rather than direct temperature, it is necessary to cover the DUT surface with black tape to obtain accurate results. The function of the black tape is to increase the emissivity of the DUT and minimize the influence of the environment.

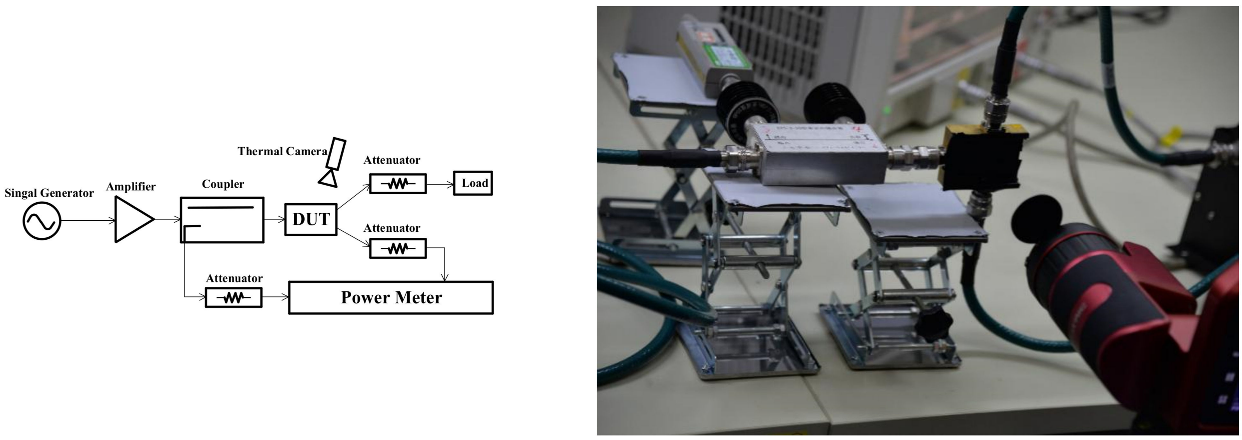

(**a**) (**b**)

Figure 6. Measurement setup for the thermal characterization of the device under test and photograph of one of the measuring devices. (**a**) Measurement setup for the thermal characterization of the device under test. (**b**) Photograph of one of the measuring devices.

In this measurement setup, a continuous signal was applied to the circuit at 2.4 GHz (center frequency). The input power was set to 10 W, 20 W, 30 W, 40 W, and 50 W, respectively.

At the moment when the signal generator was switched on, the thermal profile of the DUT was recorded. The ambient temperature was maintained at 26 °C during the experiment.

Figure 7 shows the thermal profiles of the traditional Gysel PCD and the proposed Gysel PCD when the input power of 50 W is just switched on. The maximum hot spot can be identified on the microstrip of the combine port as predicted. For the traditional Gysel PCD, the temperature variation (temperature difference between the maximum temperature of the microstrip of the circuit and the ambient temperature) caused by the input power is ΔT_T = 23.2 °C. For the proposed Gysel PCD, the temperature variation caused by the input power is ΔT_P = 10.1 °C.

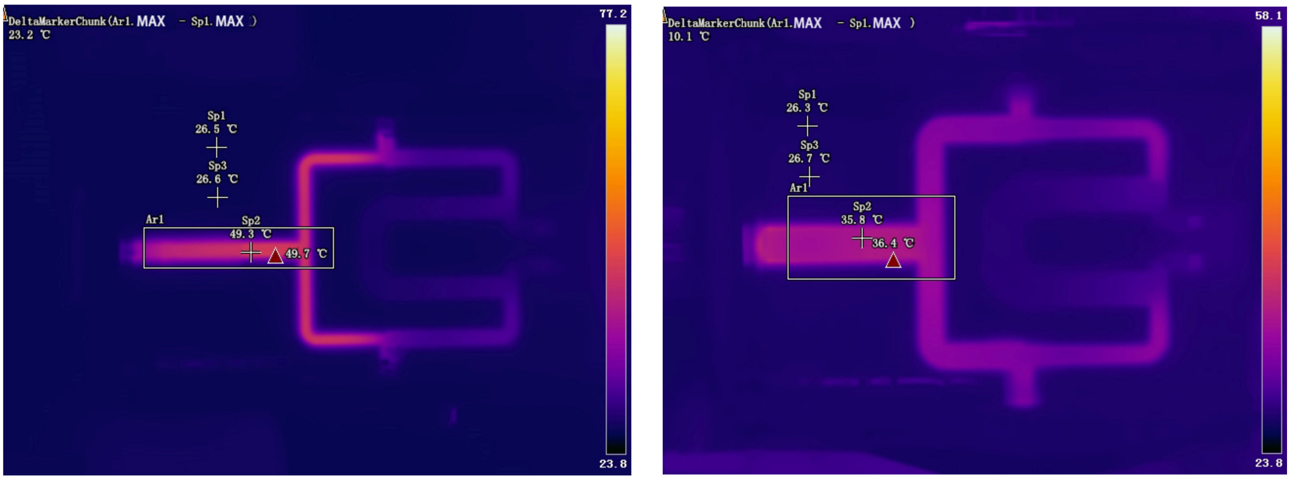

(**a**) (**b**)

Figure 7. The thermal profiles of the traditional Gysel PCD and the proposed Gysel PCD when the input power of 50 W is just switched on. (**a**) The thermal profiles of the traditional Gysel PCD. (**b**) The thermal profiles of the proposed Gysel PCD.

Figure 8 shows the temperature variation ΔT_T and the temperature variation ΔT_P at different input powers. The measurements show that when the input power is the same, ΔT_T is at least twice as high as ΔT_P. Since the T_{max} of the fabricated traditional Gysel PCD and the fabricated proposed Gysel PCD are the same, combined with (4), it can be found that the APHC of the proposed Gysel PCD is at least twice that of the traditional Gysel PCD.

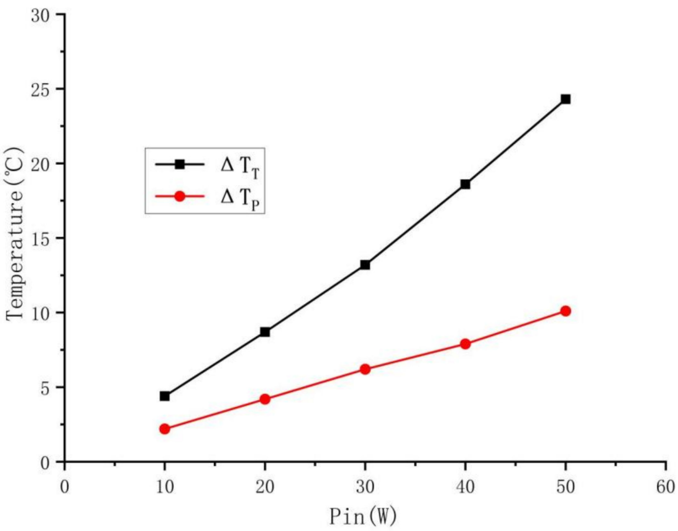

Figure 8. The ΔT_T and the ΔT_P at different input powers.

4. Conclusions

A proposed Gysel PCD with high APHC was designed, fabricated, and measured. One traditional PCD was also fabricated to compare the APHC of the proposed PCD and the traditional PCD. The temperature variation of the traditional Gysel PCD is at least twice that of the proposed Gysel PCD at the same input power, which suggests that the APHC of the fabricated proposed Gysel PCD is nearly twice that of the traditional Gysel PCD. This approach can also be applied to a Gysel PCD consisting of multiple layers of microstrip lines.

Author Contributions: Conceptualization, C.F., T.H. and W.F.; methodology, C.F. and W.H.; software, C.F.; validation, C.F., T.H. and W.F.; formal analysis, C.F. and R.F.; investigation, C.F. and T.H.; resources, Y.Z.; data curation, L.W.; writing—original draft preparation, C.F. and W.F.; writing—review and editing, C.F., W.H. and R.F.; visualization, C.F. and Y.C.; supervision, Y.C.; project administration, Y.Z.; funding acquisition, W.H. All authors have read and agreed to the published version of the manuscript.

Funding: This research received no external funding.

Data Availability Statement: Not applicable.

Conflicts of Interest: The authors declare no conflict of interest.

References

1. Gysel, U.H. A New N-Way Power Divider/Combiner Suitable for High-Power Applications. In Proceedings of the 1975 IEEE-MTT-S International Microwave Symposium, Palo Alto, CA, USA, 12–14 May 1975; pp. 116–118.
2. Zhu, Z.; Wang, Z.; Fu, Y.; Fang, S.; Liu, H.; Chen, Z.N. Unlimited Power Division Ratio of Microstrip Balanced-to-Unbalanced Gysel-Type Arbitrary Power Divider. *Electronics* **2020**, *9*, 1124. [CrossRef]
3. Shahi Gharehaghaji, H.; Shamsi, H. Design of Unequal Dual Band Gysel Power Divider With Isolation Bandwidth Improvement. *IEEE Microw. Wirel. Compon. Lett.* **2017**, *27*, 138–140. [CrossRef]
4. He, J.; Luo, W.; Chen, S. A Gysel Power Divider with Enhanced Isolation Bandwidth. In Proceedings of the 2015 Asia-Pacific Microwave Conference (APMC), Nanjing, China, 6–9 December 2015; Volume 3, pp. 1–3.
5. Lin, F.; Chu, Q.-X.; Gong, Z.; Lin, Z. Compact Broadband Gysel Power Divider with Arbitrary Power-Dividing Ratio Using Microstrip/Slotline Phase Inverter. *IEEE Trans. Microw. Theory Tech.* **2012**, *60*, 1226–1234. [CrossRef]
6. Gupta, K.C.; Garg, R.; Bahl, I.; Bhartia, P. *Microstrip Lines and Slotlines*; Artech House: London, UK, 2013; p. 7.
7. Bahl, I.J.; Gupta, K.C. Average Power-Handling Capability of Microstrip Lines. *IEE J. Microw. Opt. Acoust.* **1979**, *3*, 1. [CrossRef]
8. Yin, W.Y.; Dong, X.T. Wideband Average Power Handling Capability of Coupled Microstrips on Polyimide and Polyimide/GaAs Substrates. *IEE Proc. Microw. Antennas Propag.* **2004**, *151*, 385. [CrossRef]
9. Yin, W.-Y.; Dong, X.; Gan, Y.B. Frequency-Dependent Maximum Average Power-Handling Capabilities of Single and Edge-Coupled Microstrip Lines on Low-Temperature Co-Fired Ceramic (LTCC) Substrates. *Int. J. RF Microw. Comput. Aided Eng.* **2006**, *16*, 103–117. [CrossRef]
10. Wu, L.-S.; Zhou, X.-L.; Yin, W.-Y.; Tang, M.; Zhou, L. Characterization of Average Power Handling Capability of Bandpass Filters Using Planar Half-Wavelength Microstrip Resonators. *IEEE Microw. Wirel. Compon. Lett.* **2009**, *19*, 686–688. [CrossRef]
11. Wu, L.-S.; Mao, J.; Yin, M.Y.; Tang, M. Average Power Handling Capability of Quarter-Wavelength Microstrip Stepped-Impedance Resonator Bandpass Filter. In Proceedings of the 2012 IEEE/MTT-S International Microwave Symposium Digest, IEEE, Montreal, QC, Canada, 17–22 June 2012; pp. 1–3.
12. Yu, M. Power-Handling Capability for RF Filters. *IEEE Microw.* **2007**, *8*, 88–97. [CrossRef]
13. Sanchez-Soriano, M.A.; Quere, Y.; Le Saux, V.; Quendo, C.; Cadiou, S. Average Power Handling Capability of Microstrip Passive Circuits Considering Metal Housing and Environment Conditions. *IEEE Trans. Compon. Packag. Manuf. Technol.* **2014**, *4*, 1624–1633. [CrossRef]
14. Bahl, I.J. Average Power Handling Capability of Multilayer Microstrip Lines. *Int. J. RF Microw. Comput. Aided Eng.* **2001**, *11*, 385–395. [CrossRef]
15. Yin, W.-Y.; Dong, X.T. Wide-Band Characterization of Average Power Handling Capabilities of Some Microstrip Interconnects on Polyimide and Polyimide/GaAs Substrates. *IEEE Trans. Adv. Packag.* **2005**, *28*, 328–336. [CrossRef]
16. Yin, W.-Y.; Dong, X.T.; Mao, J.; Li, L.W. Average Power Handling Capability of Finite-Ground Thin-Film Microstrip Lines over Ultra-Wide Frequency Ranges. *IEEE Microw. Wirel. Compon. Lett.* **2005**, *15*, 715–717. [CrossRef]
17. Yin, W.-Y.; Kang, K.; Mao, J.-F. Electromagnetic-Thermal Characterization of on On-Chip Coupled (A)Symmetrical Interconnects. *IEEE Trans. Adv. Packag.* **2007**, *30*, 851–863. [CrossRef]
18. Fahmi, M.M.; Ruiz-Cruz, J.A.; Mansour, R.R. Compact Ridge Waveguide Gysel Combiners for High-Power Applications. *IEEE Trans. Microw. Theory Tech.* **2019**, *67*, 968–977. [CrossRef]

19. Guan, J.; Zhang, L.; Sun, Z.; Leng, Y.; Peng, Y. Designing Power Divider by Combining Wilkinson and Gysel Structure. *Electron. Lett.* **2012**, *48*, 769. [CrossRef]
20. Oraizi, H.; Sharifi, A.-R. Optimum Design of a Wideband Two-Way Gysel Power Divider With Source to Load Impedance Matching. *IEEE Trans. Microw. Theory Tech.* **2009**, *57*, 2238–2248. [CrossRef]